

1
2
3
4
5
6

Energy Deposition in Polymers

Matthew J. Urffer
December 2, 2012

Todo list

| | |
|-------------------------------|----|
| Expand this section | 10 |
| Get URL to work | 12 |

| | | |
|----|---|-----------|
| 7 | Contents | |
| 8 | 1 Introduction | 6 |
| 9 | 2 Previous Work | 7 |
| 10 | 2.1 Spectra Measurements | 7 |
| 11 | 2.2 Single Collision Energy Loss | 7 |
| 12 | 3 Introduction to GEANT4 | 10 |
| 13 | 3.1 Organization of the GEANT4 Toolkit | 10 |
| 14 | 3.2 GEANT4 Tracking and Secondaries | 10 |
| 15 | 4 Methods | 12 |
| 16 | 4.1 GEANT4 Implementation | 12 |
| 17 | 4.1.1 Detector Geometry | 12 |
| 18 | 4.1.2 Physics Lists | 13 |
| 19 | 4.1.3 Primary Event Generator | 15 |
| 20 | 4.2 Sensitive Detectors and Hits | 15 |
| 21 | 4.3 Analysis | 17 |
| 22 | 4.4 Determination of Energy Deposition | 18 |
| 23 | 5 Simulation Validation | 22 |
| 24 | 5.1 Energy Deposition Validation | 22 |
| 25 | 5.2 Spectra Validation | 22 |
| 26 | 6 Results | 25 |
| 27 | 6.1 Energy Deposition | 25 |
| 28 | 6.2 Secondary Electron Energy Distribuion | 26 |
| 29 | 7 Conclusions | 28 |

30 List of Figures

| | | | |
|----|----|---|----|
| 31 | 1 | Spectra properties as a function of film thickness | 7 |
| 32 | 2 | Gamma intrinsic efficiency (dashed lines) plotted against neutron counts (solid) | 8 |
| 33 | 3 | Single-collision energy loss spectra for electrons in water [4] | 9 |
| 34 | 4 | Average and median energy transfer in liquid water as functions of incident-electron energy [4] | 9 |
| 35 | 5 | World, Calorimeter, Layer and Absorber and Gap | 14 |
| 36 | 6 | 10 Layer Detector with a simulated gamma event | 21 |
| 37 | 7 | Single Collision Energy Loss of Water | 22 |
| 38 | 8 | Gamma Simulation Agreement | 23 |
| 39 | 9 | Neutron Simulation Agreement | 24 |
| 40 | 10 | Simulated Energy Depositon for a Single Film (gammas) | 25 |
| 41 | 11 | Simulated Energy Depositon for a Single Film (neutrons) | 26 |
| 42 | 12 | Simulated kinetic energies of electrons from ^{60}Co interactions | 27 |
| 43 | 13 | Comparison between average neturon and gamma energy deposition | 28 |

44 List of Tables

| | | | |
|----|---|---|---|
| 45 | 1 | Replacement Detector Requirements [3] | 6 |
| 46 | 2 | Maximum Energy of Secondary Electrons from Compton Scattering | 6 |

47 Listings

| | | | |
|----|----|--|----|
| 48 | 1 | Tracking Example | 11 |
| 49 | 2 | World Physical Volume | 12 |
| 50 | 3 | Calorimeter Volume | 12 |
| 51 | 4 | Layer Volume | 13 |
| 52 | 5 | Absorber and Gap Volumes | 13 |
| 53 | 6 | Implemented Physics List | 14 |
| 54 | 7 | Implemented Physics List | 14 |
| 55 | 8 | Primary Event Generator | 15 |
| 56 | 9 | Generate Primaries | 15 |
| 57 | 10 | Calorimeter Hit | 16 |
| 58 | 11 | Sensitive Detector | 16 |
| 59 | 12 | Creating Sensitive Detectors | 17 |
| 60 | 13 | Event Action | 18 |
| 61 | 14 | Run Action | 18 |
| 62 | 15 | Process Hit Collection | 18 |
| 63 | 16 | Run Macro | 19 |

1 Introduction

A typical day in 2011 saw 932,456 people enter into the U.S. (258,191 by air 48,073 by sea, and 621,874 by land) in addition to 64,483 truck, rail and sea containers and 253,821 privately-owned vehicles [1]. Any one of these could be a pathway of special nuclear material to enter the U.S. The interdiction of special nuclear material is desirable before the materials enters into the transportation infrastructure of the U.S. and interdiction becomes more complex. Radiation Portal Monitors (RPMs) are passive radiation detection systems implemented at over a thousand border crossings designed to determine if cargo contains any nuclear material in a safe, nondestructive and effective manner[2]. The Department of Homeland Security (DHS) continues to fund research through the Domestic Nuclear Detection Office (DNDO) in order to develop replacement technologies for the current ^3He RPMs as ^3He cannot be economically replaced. There are several alternatives to ^3He being considered, and all, with the exception of gas filled proportional detectors, involve the detection of neutrons from scintillation events of the energy deposited in the material from the neutron absorption reaction. These detectors (among other requirements outline in Table 1) must be able to effectively discriminate between gamma (which can occur in medical isotopes) and neutrons (indictive of special nuclear material).

Table 1: Replacement Detector Requirements [3]

| Parameter | Specification |
|---|--|
| Absolute neutron detection efficiency | 2.5 cps/ng of ^{252}Cf |
| Intrinsic gamma-neutron detection efficiency | $\epsilon_{int,\gamma n} \leq 10^{-6}$ |
| Gamma absolute rejection ratio for neutrons (GARRn) | $0.9 \leq \text{GARRn} \leq 1.1$ at 10 mR/h exposure |
| Cost | \$ 30,000 per system |

Neutron detectors often utilize a material doped with an isotope of large thermal cross section for absorption such as ^6Li or ^{10}B . When these materials absorb a neutron the nucleus of the isotope becomes unstable and fissions into reaction products. These reaction products (having an initial kinetic energy from the Q-value of the neutron absorption reaction) travel through the material, transferring their kinetic energy to the material. Photon interactions in the detector occur when a photon scatters off a single electron in a Compton scattering event (Table 2). This Compton electron then produces a cascade of secondary electrons in the material, which, depending upon the energy, may or may not deposit a majority of its energy in the detector. The difference in the transfer of kinetic energy from charged particle to electrons and from photon interactions (Compton scattering) to electrons introduces an opportunity to exploit the difference in energy deposition in order to maximize the discrimination between neutron and photon interactions in a detector.

Table 2: Maximum Energy of Secondary Electrons from Compton Scattering

| | Photon Energy (MeV) | Maximum Compton Energy (MeV) |
|-------------------|---------------------|------------------------------|
| ^{137}Cs | 0.662 | 0.478 |
| ^{60}Co | 1.17, 1.33 | 0.960, 1160 |

This document is organized as follows. A brief overview of the interaction of charged particles in matter will be provided in Section 2, as well as some preliminary experiments demonstrating the range of secondary electrons in neutron-gamma discrimination. The GEANT4 toolkit was used for the modeling of the energy deposition. Section 3 will provide an overview of the GEANT4 toolkit. Section 4 will provide details on how the GEANT4 toolkit was implemented for this particular simulation, as well as providing validation of the calculations performed by the GEANT4 toolkit in Section 5. In Section 6 the results of this model applied to a single film will demonstrate the enhanced ability of neutron-gamma discrimination through secondary electrons.

2 Previous Work

Previous work on the energy deposition of thin films focused on spectra measurements from fabricated films along with single collision energy loss spectra for physical insights. A sequence of 10% ^6LiF , 5% PPO-POPOP films in a PS matrix cast to thickness between 15 and 600 μm were fabricated and the response was measured from a gamma source as well as a neutron source. These experiment results are shown in 2.1. The single collision energy loss spectra was investigated for electrons in water in order to provide insight on the amount of energy an electron loses in a collision. These results are discussed in Section 2.2.

2.1 Spectra Measurements

Evidence that the secondary electrons contribute to energy loss can be seen in Figure 1 where there is an increase in the endpoint of the spectra as films become thicker. This increase in the spectra endpoint is indicative of the film producing more light, and as the light collection geometry remained constant, the increase in the endpoint is attributed to a larger energy deposition in the 50 μm film compared to the 15 μm or 25 μm film. Figure 2 shows the intrinsic efficiency of these film from spectra obtained from a ^{60}Co

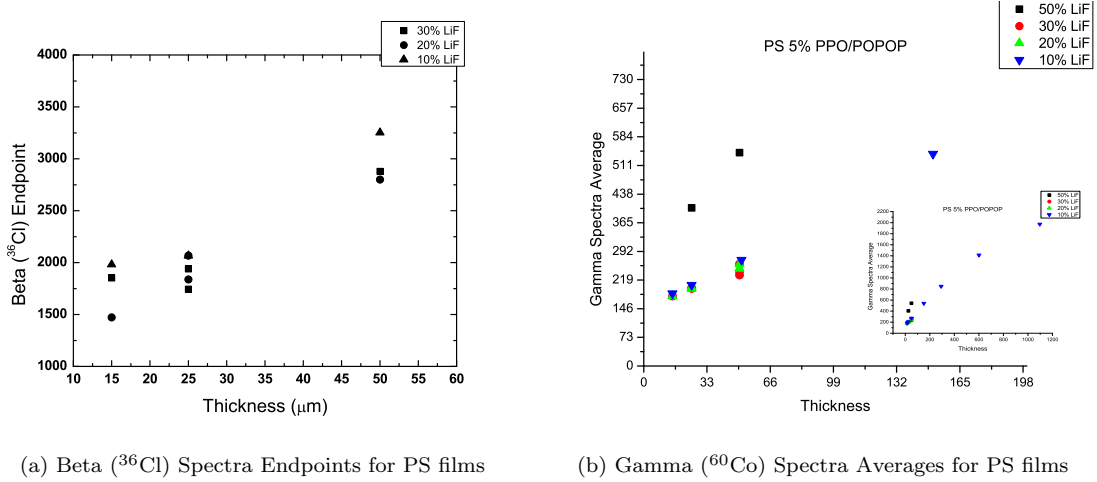


Figure 1: Spectra properties as a function of film thickness

source. As the film thickness increases the pulse height discriminator at which an intrinsic efficiency of one in a million ($\epsilon_{int,\gamma} \leq 10^{-6}$) is reached also increases. The neutron spectra (shown in the solid lines) does not increase in light yield with increasing thickness, further providing an indication that the thickness of the films can be optimized to maximize the neutron count rates¹ while minimizing the response of the detector to photons.

2.2 Single Collision Energy Loss

Single collision energy loss spectra provides the probability that that a given collision will result in an energy loss. Provided a spectra of secondary electrons from either the Compton scattered electron or the ^6Li reaction products it is then possible to determine the average energy loss per collision. A single collision energy loss spectra for water is shown in Figure 3. For low electron energies (< 50 eV) it is very probable that the electron will lose a majority of its energy in a single collision. More energetic electrons, however, tend to lose a lower fraction of there total energy. A Compton scattered photon, with an energy in the 100's of keV range, will then lose far less energy per collision than an electron in the low keV range liberated from the passage of a neutron reaction product through the material. When the average and median energy transfer are plotted as a function of incident electron energy (Figure 4) the difference in the energy loss spectra becomes more

¹The neutron count rate is increased with thickness by the increased mass of the detector

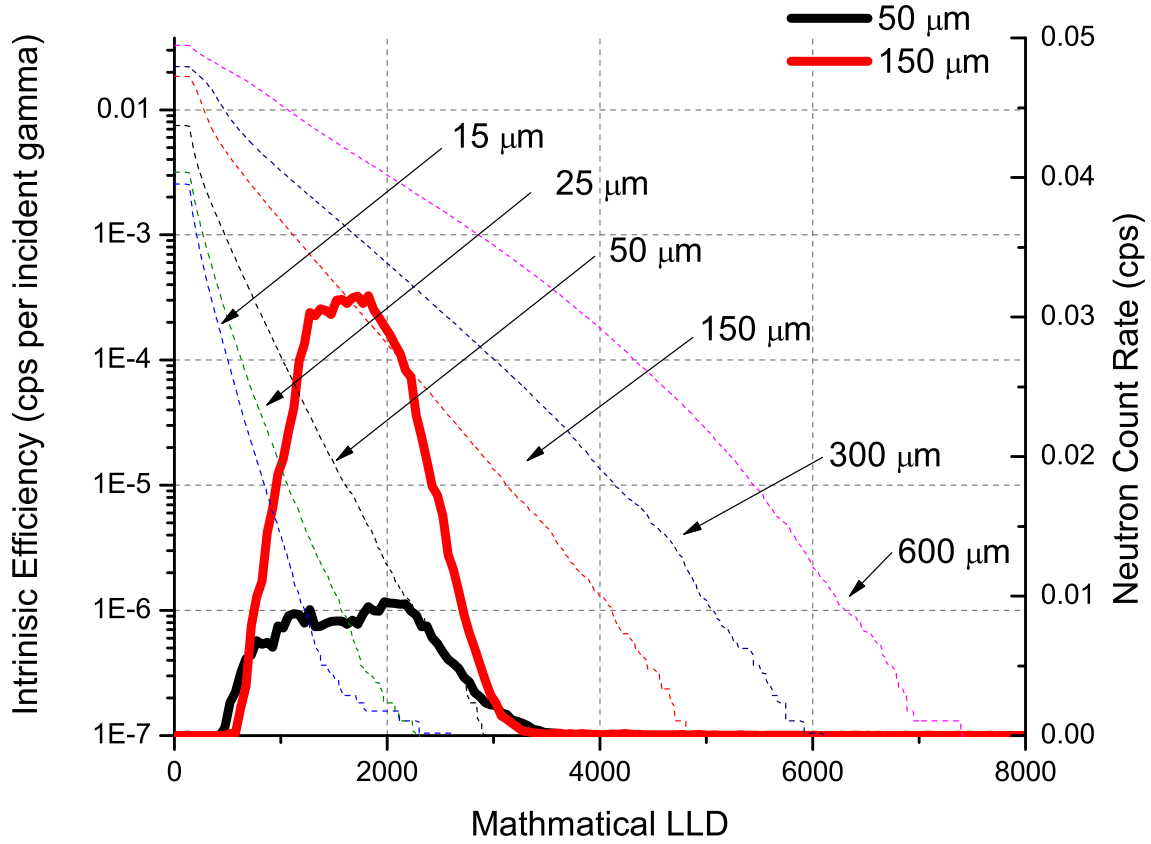


Figure 2: Gamma intrinsic efficiency (dashed lines) plotted against neutron counts (solid)

apparent. For low energies (up to an incident electron energy of 100 eV) the average and median energy transfer are roughly equal to each other, about half of the incident electron. Past 100 eV average energy increases faster than the median energy transfer implying that while a few collisions result in large energy transfers most of the collisions do not. It is also interesting to note that the average and median do not increase linearly with the incident energy past 100 eV (the ordinate axis is a log scale). In fact, the average energy transferred per collision is mostly bounded by 60 eV even for incident electron energies of 10 keV. This is significant because it implies that high energy electrons from photon events will deposit a small fraction of their energy in the material.

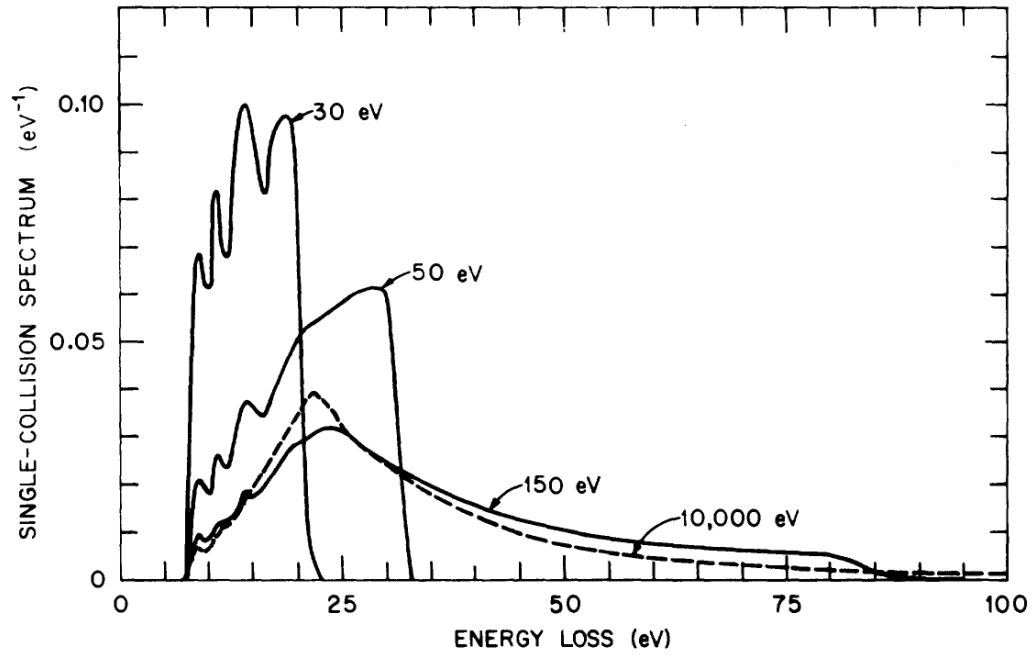


Figure 3: Single-collision energy loss spectra for electrons in water [4]

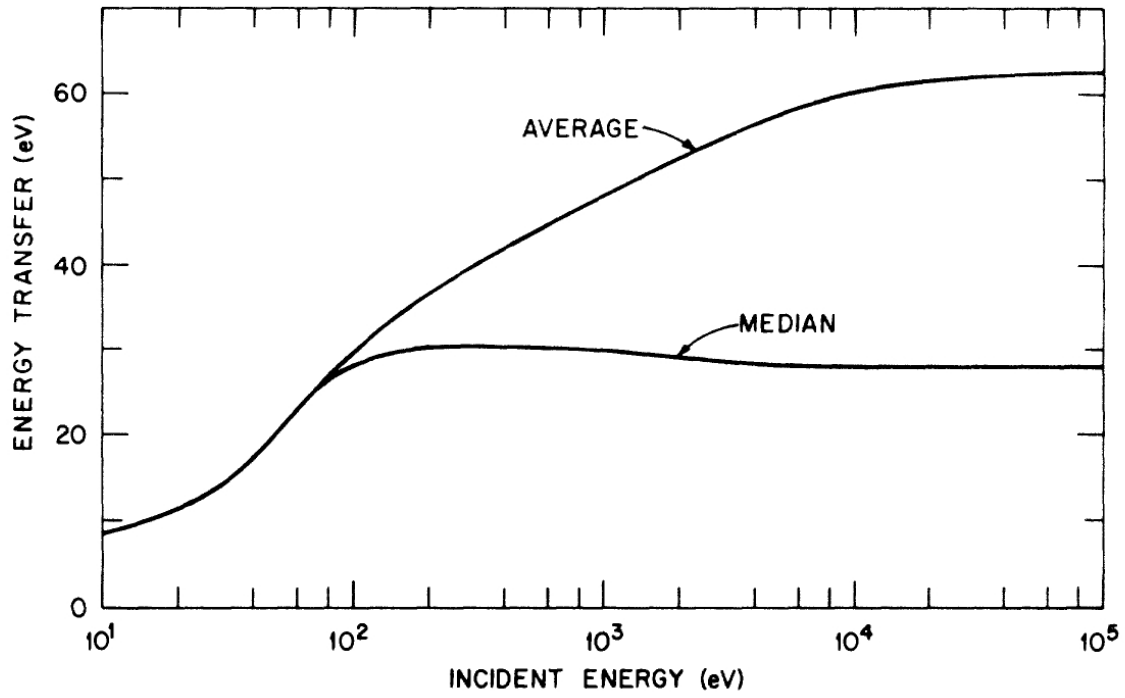


Figure 4: Average and median energy transfer in liquid water as functions of incident-electron energy [4]

3 Introduction to GEANT4

GEANT4 (GEometry ANd Tracking) is a free, open source, Monte Carlo based physics simulation toolkit developed and maintained at CERN widely used in the physics community [5, 6, 7]. It is based off of the existing FORTRAN based GEANT3, but updated to an object-oriented C++ environment based on an initiative started in 1993. The initiative grew to become an international collaboration of researchers participating in a range of high-energy physics experiments in Europe, Japan, Canada and the United States. As GEANT4 is a toolkit primarily developed for high energy physics, particles are designated according to the PDG (Particle Data Group) encoding. In addition, the physics processes are referenced according to the standard model. In the standard model particles are divided into two families, bosons (the force carriers such as photons) and fermions (matter). The fermions consist of both hadrons and leptons. Hadrons are particles composed of quarks which are divided into two classes: baryons (three quarks) and mesons (two quarks). Typical baryons include the neutron and the proton, while an example of a meson is the pion. An example of a lepton is the electron.

3.1 Organization of the GEANT4 Toolkit

The GEANT4 toolkit is divided into eight class categories:

- Run and Event - generation of events and secondary particles.
- Tracking and Track - transport of a particle by analyzing the factors limiting the step size and by applying the relevant physics models.
- Geometry and Magnetic Field - the geometrical definition of a detector (including the computation of the distances to solids) as well as the management of magnetic fields.
- Particle Definition and Matter - definition of particles and matter.
- Hits and Digitization - the creation of hits and their use for digitization in order to model a detector's readout response.
- Visualization - the visualization of a simulation including the solid geometry, trajectories and hits.
- Interface - the interactions between the toolkit and graphical user interfaces and well as external software.

There are then three classes which must be implemented by the user in order to use the toolkit. These classes are:

- `G4VUserDetectorConstruction` which defines the geometry of the simulation,
- `G4VUserPhysicsList` which defines the physics of the simulation, and
- `G4VUserPrimaryGeneratorAction` which defines the generation of primary events.

Five additional classes are available for further control over the simulation:

- `G4UserRunAction` which allows for user actions

3.2 GEANT4 Tracking and Secondaries

A GEANT4 simulation starts with a run which contains a set number of events. An event is particular process of interest to the user, such as shooting a single particle at a detector. Typical usage might be to have a run firing 1,000 neutrons at a detector, where each neutron is a single event. Each particle transported in GEANT4 is assigned a unique track ID and a parent ID. The particle that initiates the event is given a parent ID of 0 and a track ID of 1. If the parent particle has a collision, and produces a secondary particle, this secondary particle is then given a parent ID of 1 (corresponding to the first secondary) and a track ID of

Expand this
section

2. Secondaries are tracked in GEANT4 utilizing a stack in which the most recent secondary (and its cascade) is tracked first.

Listing 1 provides an example from the verbose output of GEANT4 of the tracking. The initial particle in the event is the neutron because it has a parent ID of 0. The alpha and triton are the secondaries produced by this collision. The alpha is assigned a parent ID of 1 (corresponding to the first generation) with a track ID of 3. The triton is also assigned a parent ID of 1, but with a track ID of 2.

Listing 1: Tracking Example

```

*****
* G4Track Information: Particle = neutron, Track ID = 1, Parent ID = 0
*****
Step#    X(mm)    Y(mm)    Z(mm) KinE(MeV)  dE(MeV)  StepLeng  TrackLeng  NextVolume  ProcName
0         0         0         -6.59  2.5e-08    0         0         0         Absorber  initStep
1         0         0         -3.64    0         0         2.95    2.95    Absorber  NeutronInelastic
:----- List of 2ndaries - #SpawnInStep= 2( Rest= 0, Along= 0, Post= 2), #SpawnTotal= 2 -----
:         0         0         -3.64    2.73          triton
:         0         0         -3.64    2.05          alpha
:----- EndOf2ndaries Info -----
*****
* G4Track Information: Particle = alpha, Track ID = 3, Parent ID = 1
*****
Step#    X(mm)    Y(mm)    Z(mm) KinE(MeV)  dE(MeV)  StepLeng  TrackLeng  NextVolume  ProcName
0         0         0         -3.64    2.05    0         0         0         Absorber  initStep
1 -0.000201 0.000128    -3.64    2.01    0.0491 0.000266 0.000266  Absorber  ionIoni
2 -0.00049 0.000312    -3.64    1.93    0.0705 0.000381 0.000647  Absorber  ionIoni
*****
* G4Track Information: Particle = triton, Track ID = 2, Parent ID = 1
*****
Step#    X(mm)    Y(mm)    Z(mm) KinE(MeV)  dE(MeV)  StepLeng  TrackLeng  NextVolume  ProcName
0         0         0         -3.64    2.73    0         0         0         Absorber  initStep
1 0.000339 -0.000215    -3.64    2.71    0.0116 0.000447 0.000447  Absorber  hIoni

```

4 Methods

A discussion of the steps necessary to implement the simulation of energy deposition in GEANT4 follows. This involved writing the code for the simulation, as well as correctly interpreting the output. As such, this section is organized by first examining the process of setting up the simulation and then will go into the analysis of the results from the toolkit.

4.1 GEANT4 Implementation

A large focus of this work was on creating a working simulation of the GEANT4 toolkit. Preliminary attempts were made to install GEANT4 on a Windows based machine linking to Microsoft Visual Studio. While these attempts were successful, a larger scale computing environment was desired. GEANT4 was then installed on the University of Tennessee's nuclear engineering computing cluster, along with the necessary visualization drivers and data files. Brief documentation on compiling simple examples on the cluster are available at necluster.engr.utk.edu/wiki/index.php/Geant4². For convenience a subversion repository was created to manage the developed code base, and all source code is available by anonymous checkout from <http://www.murphs-code-repository.googlecode.com/svn/trunk/layeredPolymerTracking>. Revision 360 was the code base used to generate the results shown. The following section provides implementation specific details of the code base used to simulate the energy deposition in thin films. It is organized according to the three base classes that a user must implement in GEANT4, namely `G4VUserDetectorConstruction`, `G4VUserPhysicsList`, and `G4VUserPrimaryGeneratorAction`.

Get URL to work

4.1.1 Detector Geometry

A detector geometry in GEANT4 is made up of a number of volumes. The largest volume is the `world` volume which contains all other volumes in the detector geometry. Each volume (an instance of `G4VPhysicalVolume`) is created by assigning a position, a pointer to the mother volume and a pointer to its mother volume (or `NULL` if it is the `world` volume). A volume's shape is described by `G4VSolid`, which has a shape and the specific values for each dimension. A volume's full properties is described by a logical volume. A `G4LogicalVolume` includes a pointer to the geometrical properties of the volume (the solid) along with physical characteristics including:

- the material of the volume,
- sensitive detectors of the volume and,
- any magnetic fields.

Listing 2 provides the implementation of the world physical volume. The geometry was set up such that it is possible to define multiple layers of detectors, as shown in Figure 6.

Listing 2: World Physical Volume

```
// World
worldS = new G4Box("World",worldSizeXY, worldSizeXY, worldSizeZ*0.5);
worldLV = new G4LogicalVolume(worldS,defaultMaterial,"World");
worldPV = new G4PVPlacement(0,G4ThreeVector(),worldLV,"World",0,false,0,fCheckOverlaps);
```

The detector was described by creating creating a single layer of neutron absorber and gap material and placing it in another volume (the calorimeter). The containing volume (calorimeter) was placed inside of the the physical world (Listing 3).

Listing 3: Calorimeter Volume

```
// Calorimeter (gap material)
caloS = new G4Tubs("Calorimeter",iRadius,oRadius,caloThickness/2,startAngle,spanAngle);
```

²It should be noted that this example uses the CMAKE build system (as per the GEANT4 recommendation) but a large majority of the examples still use GNUMake for building. This can be accomplished by adding `source /opt/geant4/geant4-9.5p1/share/Geant4-9.5.1/geant4make/geant4make.sh` to the user's `.bashrc`.

```

252 caloLV = new G4LogicalVolume(caloS, gapMaterial, "Calorimeter");
253 4 caloPV = new G4PVPlacement(0, G4ThreeVector(), caloLV, "Calorimeter", worldLV, false, 0,
254     fCheckOverlaps);
255

```

256 The `calorimeter` was the mother volume for each layer. The code was developed such that the simulation of
 257 multiple layers can be easily set at compile time or by utilizing a run macro through the `DetectorMessenger`
 258 class. Multiple repeated volume can be achieved in GEANT4 through `G4PVReplica` or `G4PVParameterised`.
 259 As each of the layers had the same geometry, `G4PVReplica` was chosen as the implementation (Listing 4).

Listing 4: Layer Volume

```

260
261 1 // Layer (Consists of Absorber and Gap)
262 layerS = new G4Tubs("Layer", iRadius, oRadius, layerThickness/2, startAngle, spanAngle);
263 3 layerLV = new G4LogicalVolume(layerS, defaultMaterial, "Layer");
264 if (nofLayers > 1){
265 5     layerPV = new G4PVReplica("Layer", layerLV, caloLV, kZAxis, nofLayers, layerThickness, -
266     caloThickness/2);
267 }else{
268 7     layerPV = new G4PVPlacement(0, G4ThreeVector(0.0, 0.0, 0.0), layerLV, "Layer", caloLV,
269     false, 0, fCheckOverlaps);
270 }

```

272 Finally, the neutron absorber and gap material were defined as single cylinders which were then placed in the
 273 layer mother volume (Listing 5). The size of these solids (and the materials) could be set either at compile
 274 time through `DetectorConstruction` constructor or by using the `DetectorMessenger` in the run macro.
 275 Figure 6 shows a rendering of the 10 layers of the detector with the trajectories from a gamma event.

Listing 5: Absorber and Gap Volumes

```

276
277 // Absorber
278 2 absS = new G4Tubs("Abso", iRadius, oRadius, absThickness/2, startAngle, spanAngle);
279 absLV = new G4LogicalVolume(absS, absMaterial, "Absorber", 0);
280 4 absPV = new G4PVPlacement(0, G4ThreeVector(0.0, 0.0, -gapThickness/2), absLV, "Absorber",
281     layerLV, false, 0, fCheckOverlaps);
282
283 6 // Gap
284 gapS = new G4Tubs("Gap", iRadius, oRadius, gapThickness/2, startAngle, spanAngle);
285 8 gapLV = new G4LogicalVolume(gapS, gapMaterial, "Gap", 0);
286 gapPV = new G4PVPlacement(0, G4ThreeVector(0.0, 0.0, absThickness/2), gapLV, "Gap", layerLV,
287     false, 0, fCheckOverlaps);
288

```

289 4.1.2 Physics Lists

290 The user of the GEANT4 toolkit is responsible for selecting the proper physics processes to model in the
 291 `PhysicsList`. This is unlike other transport codes (such as MCNPX) where basic physics are enabled by
 292 default and the user only has select the appropriate cards. However, GEANT4 does provide examples of
 293 implemented `PhysicsLists` as well as modular physics lists which provide a way to construct a physics list by
 294 combing physics list. Thus, extensive use of `G4ModularPhysicsList` was employed to handle the assigning
 295 of the physics processes to each particle in the correct order. The physics lists chosen for this simulation are
 296 listed below:

- 297 • **G4EmStandardPhysics** The electromagnetic physics defines the electrons, muons, and taus along with
 298 their corresponding neutrinos. For electrons, the primary concern of this simulation, multiple scattering,
 299 electron ionization, and electron bremsstrahlung processes were assigned. In addition the positron is
 300 defined and the multiple scattering process, electron ionization process, electron bremsstrahlung process
 301 and positron annihilation is assigned [8].
- 302 • **G4EmLivermorePhysics** The Livermore physics process extend the `EMStandardPhysics` down to low
 303 (250 eV) energies. Even lower energies can be reached by including `G4DNAPhysics`. The physics
 304 processes extended with `G4EmLivermorePhysics` are the photo-electric effect, Compton scattering,
 305 Rayleigh scattering, gamma conversion, Ionisation and Bremsstrahlung[8].

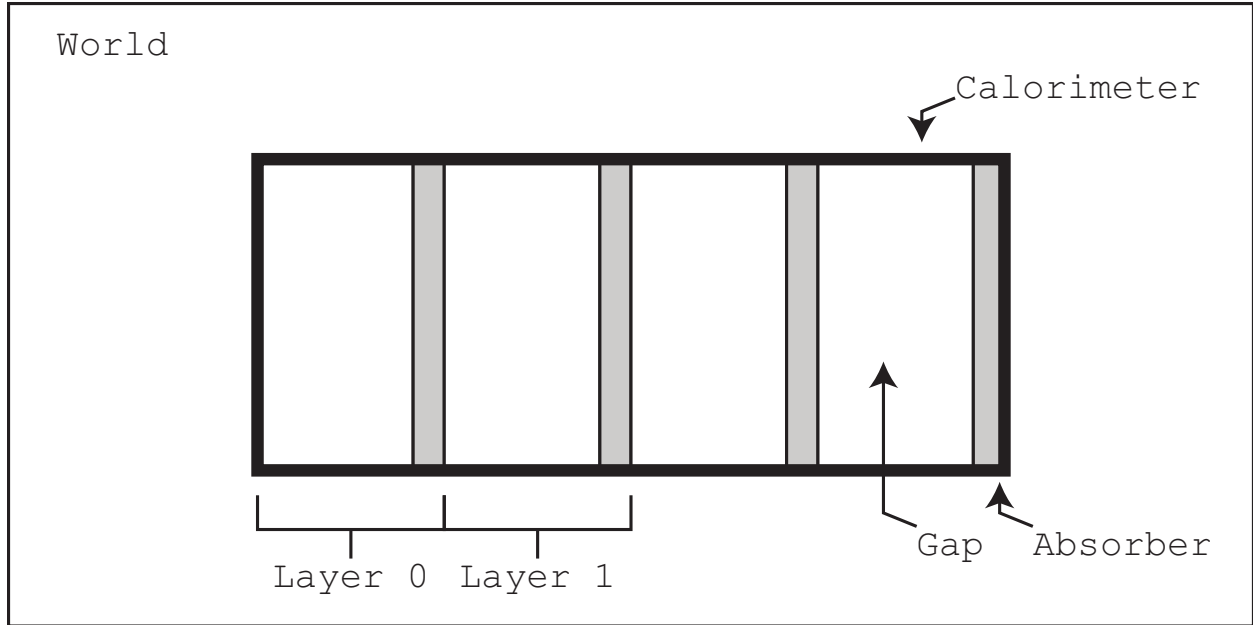


Figure 5: World, Calorimeter, Layer and Absorber and Gap

- **HadronPhysicsQGSP_BERT_HP** Hadronic physics are included to model the nuclear interactions. The chosen list is a Quark Gluon String Model for energies in the 5-25 GeV range, with a Bertini cascade model until 20 MeV. Once a hadron has an energy of 20 MeV the high precision cross section driven models are applied[9].
- **G4IonPhysics** Finally, to handle the transport of the charged ions resulting from an ${}^6\text{Li}(n, \alpha){}^3\text{H}$ interaction the **G4IonPhysics** list was used.

Listing 6: Implemented Physics List

```

312 /**
313  * PhysicsList
314  *
315  * Constructs the physics of the simulation
316  */
317 PhysicsList::PhysicsList() : G4VModularPhysicsList() {
318     currentDefaultCut = 10*nm;
319
320     // Adding Physics List
321     //RegisterPhysics( new G4EmDNAPhysics());
322     RegisterPhysics( new G4EmStandardPhysics());
323     RegisterPhysics( new G4EmLivermorePhysics());
324     RegisterPhysics( new HadronPhysicsQGSP_BERT_HP());
325     RegisterPhysics( new G4IonPhysics());
326 }
327
328 
```

Finally, the default cut range was decreased from 1 cm to 1 nm in **SetCuts()** (Listing 7)

Listing 7: Implemented Physics List

```

330 void PhysicsList::SetCuts(){
331     SetDefaultCutValue(10*nm);
332 }
333
334 
```

4.1.3 Primary Event Generator

The user is responsible for telling the simulation toolkit the primary event to generate. While there is great flexibility to generate any source distribution, a particle gun was chosen for simplicity. `G4ParticleGun` generates primary particle(s) with a given momentum and position without any randomization. The implementation of this is shown in Listing 8.

Listing 8: Primary Event Generator

```
PrimaryGeneratorAction::PrimaryGeneratorAction() : G4VUserPrimaryGeneratorAction(),
    fParticleGun(0) {
    G4int nofParticles = 1;
    fParticleGun = new G4ParticleGun(nofParticles);

    // default particle kinematic
    G4ParticleDefinition* particleDefinition = G4ParticleTable::GetParticleTable()->
        FindParticle("e-");
    fParticleGun->SetParticlePosition(G4ThreeVector(0.,0.,0.0));
    fParticleGun->SetParticleDefinition(particleDefinition);
    fParticleGun->SetParticleMomentumDirection(G4ThreeVector(0.,0.,1.));
    fParticleGun->SetParticleEnergy(50.*MeV);
}
```

Actual primary particles are generated with `GeneratePrimaries`, which uses the `G4ParticleGun` to determine the vertex of the primary event.

Listing 9: Generate Primaries

```
void PrimaryGeneratorAction::GeneratePrimaries(G4Event* anEvent)
{
    // This function is called at the beginning of event

    // In order to avoid dependence of PrimaryGeneratorAction
    // on DetectorConstruction class we get world volume
    // from G4LogicalVolumeStore
    G4double worldZHalfLength = 0;
    G4LogicalVolume* worlLV = G4LogicalVolumeStore::GetInstance()->GetVolume("World");
    G4Box* worldBox = 0;
    if ( worlLV ) worldBox = dynamic_cast< G4Box*>(worlLV->GetSolid());
    if ( worldBox ) {
        worldZHalfLength = worldBox->GetZHalfLength();
    }
    else {
        G4cerr << "World volume of box not found." << G4endl;
        G4cerr << "Perhaps you have changed geometry." << G4endl;
        G4cerr << "The gun will be place in the center." << G4endl;
    }

    // Set gun position
    fParticleGun->SetParticlePosition(G4ThreeVector(0., 0., -worldZHalfLength+1*cm));
    fParticleGun->GeneratePrimaryVertex(anEvent);
}
```

4.2 Sensitive Detectors and Hits

GEANT4 offers a myriad of different ways to output the results of a simulation. It is possible to write out every track with the `Verbose = 1` option, create `MultiFunctionalDetector` and `G4VPrimitiveScorer`, or implement a hit and readout based approach [10]. Previous GEANT4 experience included `G4VHit` and `G4VSensitiveDetector`, so this approach was used in this simulation. A hit is defined to be a snapshot of the physical interaction of a track in a sensitive region of a detector. As the user is responsible for implementing `G4VHit` the hit can contain any information about the step, including:

- the position and time of the step,
- the momentum and energy of the track,

- the energy deposition of the step,
- or information about the geometry.

For this simulation any information about the particle that could be recorded was recorded. This included the energy deposition, position of the hit, momentum, kinetic energy, track ID, parent ID, particle definition, volume and copy number (Listing 10).

Listing 10: Calorimeter Hit

```

397 /**
398  * @brief - Hit: a snapshot of the physical interaction of a track in the sensitive region
399  * of a detector
400  *
401  * Contains:
402  * - Particle Information (type and rank (primary, secondary, tertiary ...))
403  * - Position and time
404  * - momentum and kinetic energy
405  * - deposition in volume
406  * - geometric information
407  */
408
409 class CaloHit : public G4VHit {
410 public:
411     CaloHit(const G4int layer);
412     ~CaloHit();
413
414     inline void* operator new(size_t);
415     inline void operator delete(void*);
416     void Print();
417
418 private:
419     G4double edep; /* Energy Deposited at the Hit */
420     G4ThreeVector pos; /* Position of the hit */
421     G4double stepLength; /* Step Length */
422     G4ThreeVector momentum; /* Momentum of the step */
423     G4double kEnergy; /* Kinetic Energy of the particle */
424     G4int trackID; /* Track ID */
425     G4int parentID; /* Parent ID */
426     G4ParticleDefinition* particle; /* Particle Definition */
427     G4int particleRank; /* Primary, Secondary, etc */
428     G4VPhysicalVolume* volume; /* Physical Volume */
429     G4int layerNumber; /* Copy Number of Layer */
430
431 public:
432     // Setter and Getters
433 };
434
435 typedef G4THitsCollection<CaloHit> CaloHitsCollection;
436 extern G4Allocator<CaloHit> HitAllocator;
437
438 inline void* CaloHit::operator new(size_t){
439     void *aHit;
440     aHit = (void *) HitAllocator.MallocSingle();
441     return aHit;
442 }
443
444 inline void CaloHit::operator delete(void *aHit){
445     HitAllocator.FreeSingle((CaloHit*) aHit);
446 }

```

The G4VSensitiveDetector is attached to a logical volume and is responsible for filling the hit collection. This is accomplished in ProcessHits of CaloSensitiveDetector (Listing 11).

Listing 11: Sensitive Detector

```

450 /**
451  * ProcessHits
452  *
453

```



```

454 4  * Adds a hit to the sensitive detector, depending on the step
455 5  */
456 6  G4bool CaloSensitiveDetector::ProcessHits(G4Step* aStep,G4TouchableHistory*){
457 7
458 8      G4double edep = aStep->GetTotalEnergyDeposit();
459 9      G4double stepLength = aStep->GetStepLength();
460 10
461 11      // Getting the copy number
462 12      G4TouchableHistory* touchable = (G4TouchableHistory*)
463 13          (aStep->GetPreStepPoint()->GetTouchable());
464 14      G4int layerIndex = touchable->GetReplicaNumber(1);
465 15
466 16      // Creating the hit
467 17      CaloHit* newHit = new CaloHit(layerIndex);
468 18      newHit->SetTrackID(aStep->GetTrack()->GetTrackID());
469 19      newHit->SetParentID(aStep->GetTrack()->GetParentID());
470 20      newHit->SetEdep(edep);
471 21      newHit->SetStepLength(stepLength);
472 22      newHit->SetPosition(aStep->GetPreStepPoint()->GetPosition());
473 23      newHit->SetLayerNumber(layerIndex);
474 24      newHit->SetMomentum(aStep->GetPreStepPoint()->GetMomentum());
475 25      newHit->SetKineticEnergy (aStep->GetPreStepPoint()->GetKineticEnergy());
476 26      newHit->SetParticle(aStep->GetTrack()->GetDefinition());
477 27      newHit->SetVolume(aStep->GetTrack()->GetVolume());
478 28
479 29      // Adding the hit to the collection
480 30      hitCollection->insert( newHit );
481 31
482 32      return true;
483 33 }

```

485 The simulation was designed so that a separate sensitive detector was assigned to the gap and absorber.
486 While this is not strictly necessary as the geometric position determines what layer of the gap or absorber
487 the hit occurred in, this made the analysis code easier to write. A separate method was written in
488 `DetectorConstruction` to create the sensitive detectors and assign them to the proper logical volumes
489 (Listing 12) `SetSensitiveDetectors()` is called from the the constructor of `DetectorConstruction`.

Listing 12: Creating Sensitive Detectors

```

490 1 /**
491 2  * SetSensitiveDetectors
492 3  *
493 4  * Setting the Sensitive Detectors of the Detector
494 5  */
495 6
496 7  void DetectorConstruction::SetSensitiveDetectors(){
497 8      G4SDManager* SDman = G4SDManager::GetSDMpointer();
498 9      absSD = new CaloSensitiveDetector("SD/AbsSD", "AbsHitCollection");
499 10      SDman->AddNewDetector(absSD);
500 11      absLV->SetSensitiveDetector(absSD);
501 12
502 13      gapSD = new CaloSensitiveDetector("SD/GapSD", "GapHitCollection");
503 14      SDman->AddNewDetector(gapSD);
504 15      gapLV->SetSensitiveDetector(gapSD);
505 16  }
506 17

```

507 4.3 Analysis

508 Analysis of hit collection was preformed with ROOT. Once again there are other options (notably Open-
509 Scientist) but previous experience was why ROOT was selected as the base for the Analysis framework. A
510 singleton class was written for the analysis which processed the hit collections, assigning the various results
511 to root histograms. User action classes `EventAction` and `RunAction` are called at the beginning and end of
512 each run and event, respectively (Listing 13,14). These classes allowed for the analysis code to be independent
513 of the simulation.

Listing 13: Event Action

```

514 EventAction::EventAction() : G4UserEventAction(){
515     // Nothing to be Done Here
516 }
517
518
519 /**
520  * BeginOfEventAction
521  *
522  * @param const G4Event* event - event to be processed
523  *
524  * At the beginning of an event we want to clear all the event
525  * accumulation variables.
526  */
527 void EventAction::BeginOfEventAction(const G4Event* event){
528     Analysis::GetInstance()->PrepareNewEvent(event);
529 }
530
531 /**
532  * EndOfEventAction
533  *
534  * @param const G4Event* event - event to be processed
535  *
536  * At the end of an event we want to call analysis to process
537  * this event, and record the useful information.
538  */
539 void EventAction::EndOfEventAction(const G4Event* event){
540     Analysis::GetInstance()->EndOfEvent(event);
541 }
542

```

Listing 14: Run Action

```

543 RunAction::RunAction() : G4UserRunAction(){ }
544
545
546 void RunAction::BeginOfRunAction(const G4Run* run){
547     G4cout<<"Starting run: " << run->GetRunID()<< G4endl;
548     Analysis::GetInstance()->PrepareNewRun(run);
549 }
550
551 void RunAction::EndOfRunAction(const G4Run* aRun){
552     Analysis::GetInstance()->EndOfRun(aRun);
553 }
554

```

4.4 Determination of Energy Deposition

The energy deposition of an event is calculated by the sum of all of the energy deposited by individual hits in the sensitive detector (Equation 4.1). While it is possible to break down the energy deposition by which physics process caused the deposition, this was not implemented in order to avoid over complication.

$$E_{\text{dep,event}} = \sum E_{\text{dep,hit}} \quad (4.1)$$

`ProcessHitCollection` is called at the end of each event (Listing 15). Each hit is accessed and the layer at which it occurs is determined³. In addition the name of the volume is determined, and the energy deposition of the hit is added to the energy deposition of the event. If the hit occurred in the **absorber** layer and the particle is an electron the kinetic energy of that hit is also recorded.

Listing 15: Process Hit Collection

```

560
561 /**
562  * ProcessHitCollection
563  *

```

³C arrays start at 0, so memory is allocated for one more than the total number of layers. This allows for `NUMLAYERS+1` to be used as an index into the histogram for the total of all layers in the material (either **gap** or **absorber**).

```

564 * @param G4VHitsCollection *hc
565 */
566 void Analysis::ProcessHitCollection(G4VHitsCollection *hc, G4int eventID){
567
568     // Looping through the hit collection
569     G4double hitColEdepTot_Abs[NUMLAYERS+1]; // Total EDep (abs) for Hit Collection
570     G4double hitColEdepTot_Gap[NUMLAYERS+1]; // Total EDep (gap) for Hit Collection
571     G4int PID; // Parent ID
572     for(int i= 0; i < NUMLAYERS+1; i++){
573         hitColEdepTot_Abs[i] = 0.0;
574         hitColEdepTot_Gap[i] = 0.0;
575     }
576
577     // Energy Deposition of the event
578     for(G4int i = 0; i < hc->GetSize(); i++){
579         CaloHit* hit = (CaloHit*) hc->GetHit(i);
580
581         G4double eDep = hit->GetEdep();
582         G4int layerNum = hit->GetLayerNumber();
583         if (strcmp(hit->GetVolume()->GetName(), "Gap")){
584             // Hit occurred in the Gap
585             hitColEdepTot_Gap[layerNum] += eDep;
586             (hHitTotEdepGap[layerNum])->Fill(eDep);
587         }else if(strcmp(hit->GetVolume()->GetName(), "Absorber")){
588             // Hit occurred in the Abs
589             hitColEdepTot_Abs[layerNum] += eDep;
590             (hHitTotEdepAbs[layerNum])->Fill(eDep);
591
592             /* Is this a secondary electron of the event? */
593             if(hit->GetParticle()->GetPDGEncoding() == 11){
594                 PID = hit->GetParentID();
595                 if (PID < NUMPID){
596                     (hSecElecKinAbs[layerNum][PID])->Fill(hit->GetKineticEnergy());
597                 }
598             }
599         }else{
600             G4cout<<"ERROR - Unkown Volume for sensitive detector"<<G4endl;
601         }
602     }
603
604     // Adding this Hit collection's energy deposited to event total
605     for (int i = 0; i < NUMLAYERS; i++){
606         // Incrementing each individual bin
607         eventEdepTot_Abs[i] += hitColEdepTot_Abs[i];
608         eventEdepTot_Gap[i] += hitColEdepTot_Gap[i];
609
610         // Last bin is Calorimeter Total (all Abs layers and all Gap layers)
611         eventEdepTot_Abs[NUMLAYERS] += hitColEdepTot_Abs[i];
612         eventEdepTot_Gap[NUMLAYERS] += hitColEdepTot_Gap[i];
613     }
614 }
615 }

```

617 Finally, a run macro was written to control the entire run (Listing 16). The material and thickness
618 of the detector are declared (made possible by the use of `DetectorMessenger`), and then the detector is
619 dynamically updated. A ^{60}Co source is simulated by shooting photons of the 1.1732 MeV and 1.3325 MeV.
620 The source particle is then changed to a neutron, and thermal (0.025 eV) neutrons are shot at the detector.
621 The thickness of the absorber is then increased, the geometry updated, and the entire process repeated. As
622 these runs tend to take a large amount of time, GEANT4 was parallelized for use with MPI to take advantage
623 of the cluster computing power.

Listing 16: Run Macro

```

624 #
625 /tracking/verbose 0
626 #
627 # Setting up the detector

```

```

629 5 #
630 /PolymerTransport/det/setAbsMat PS_Detector
631 7 /PolymerTransport/det/setGapMat G4_POLYSTYRENE
632 /PolymerTransport/det/setGapThick 0.3175 cm
633 9 #
634 /PolymerTransport/det/setAbsThick 15 um
635 1 /PolymerTransport/det/update
636 # Cobalt 60
637 3 /gun/particle gamma
638 /gun/direction 0 0 1
639 5 /gun/energy 1.1732 MeV
640 /run/beamOn 500000000 # 500 Million
641 7 /gun/energy 1.3325 MeV
642 /run/beamOn 500000000 # 500 Million
643 9 # Neutron
644 /gun/particle neutron
645 1 /gun/energy 0.025 eV
646 /run/beamOn 1000000 # 1 Million
647 3 #
648 /PolymerTransport/det/setAbsThick 25 um
649 5 /PolymerTransport/det/update
650 7

```

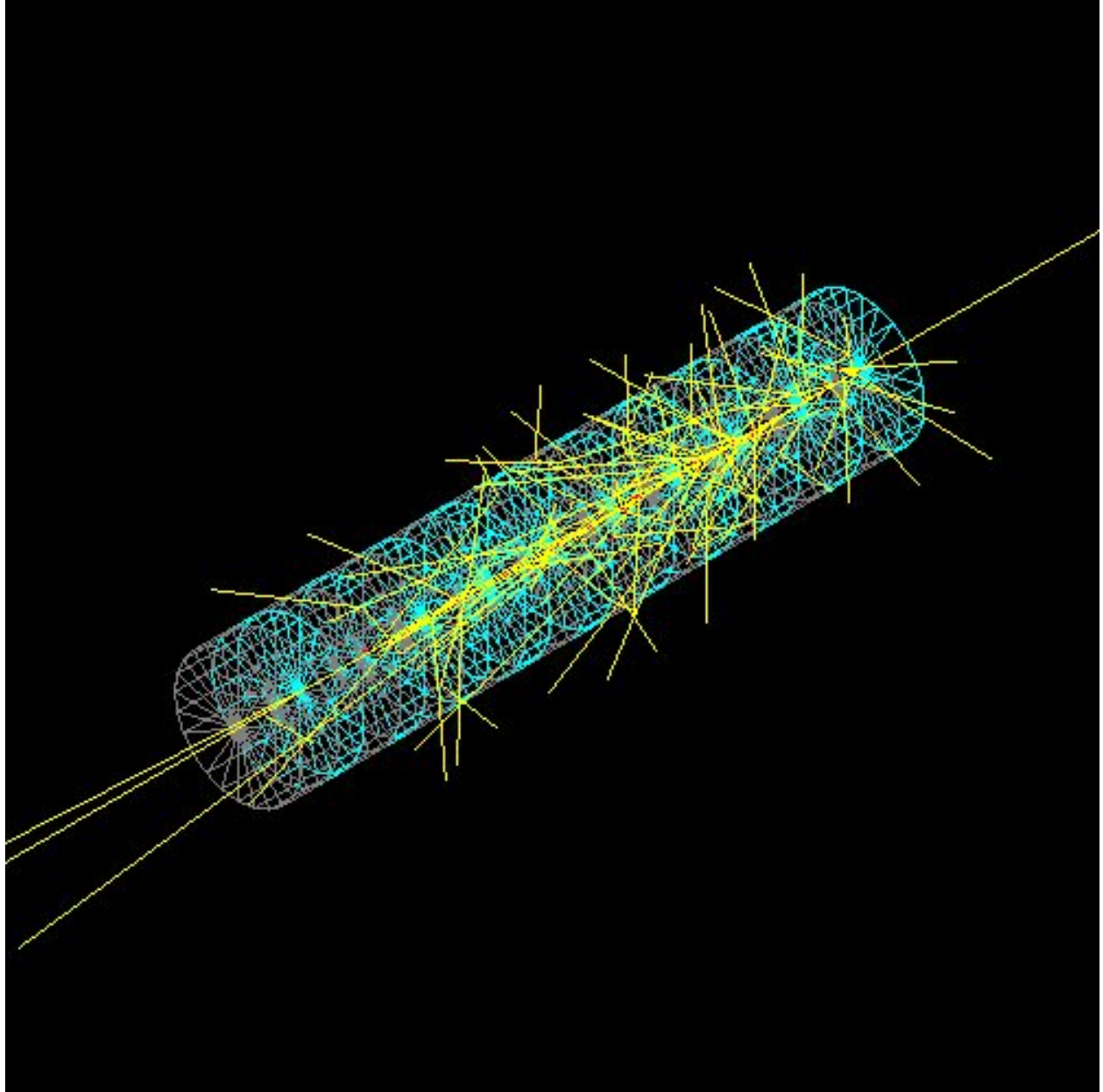


Figure 6: 10 Layer Detector with a simulated gamma event

5 Simulation Validation

GEANT4 is a toolkit implemented by the user so extensive efforts were completed in order to validate the results and ensure no bugs exists. First steps were taken (for small runs) to compute the energy deposition for small runs by hand in order to make sure they agreed with the analysis code. In addition the reaction products of the ${}^6\text{Li}(n, \alpha){}^3\text{H}$ were checked to make sure that they agreed with the published values ⁴. The GEANT4 simulation was validated by comparing the single collision energy loss spectra in water and by comparing the simulation energy deposition to that of a measured spectra.

5.1 Energy Deposition Validation

The energy deposition was tested by reproducing the single collision energy loss spectra in water⁵. The PhysicsList was extended to include G4DNAPhysics and the detector material was set to the NIST definition contained in the toolkit with `G4Material* H2O = man->FindOrBuildMaterial("G4_WATER")`. In general there was excellent agreement between the simulated energy spectra and a previously published spectra[4]. The simulated spectra had much better resolution at fine energies (corresponding to discrete states) of which Turners did not.

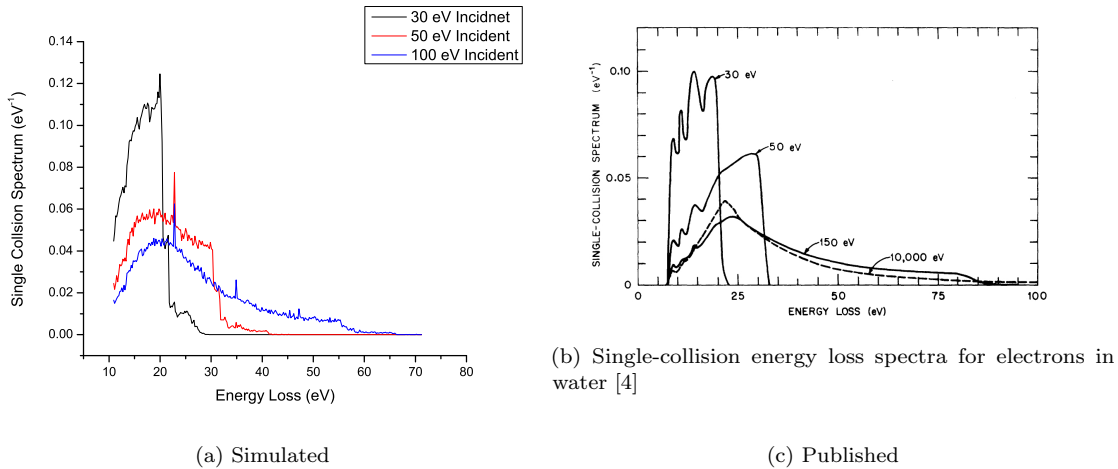


Figure 7: Single Collision Energy Loss of Water

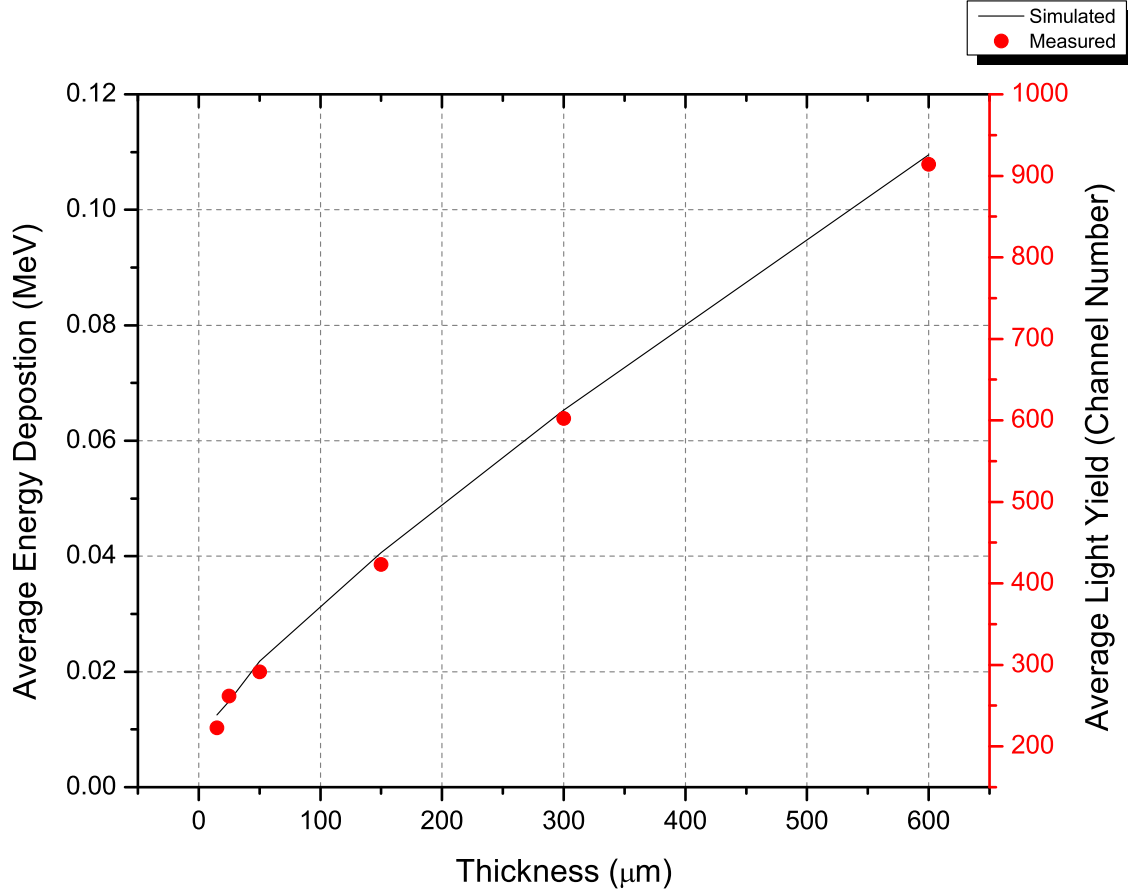
5.2 Spectra Validation

The simulated energy deposition is not the directly equivalent to light collected on the PMT because the scintillation process and light collection is not modeled. However, it is well known that scintillation follows the energy deposition[11]. Thus, up to scaling constants, the energy deposition can be considered equivalent to the scintillation and representative of the measured spectra. Rather than attempting to back out these scaling constants the weighted average of spectra were used in which integration and normalization removes these fudge factors. The simulation was validated by computing the weighted average of the energy deposition 5.1 and comparing it to the spectra average defined in 5.2. There is excellent agreement between the measured gamma weighted average (right ordinate axis) and the average energy deposition from a ${}^{60}\text{Co}$ source (left

⁴GEANT4 4.9.2.p01 contains an error in which extra photons are generated, <http://hypernews.slac.stanford.edu/HyperNews/geant4/get/phys-list/530.html>. This has been fixed in the release used, 4.9.5p1

⁵An analysis class was not written for this simulation. Instead the verbosity of the simulation was set to `verbose=1` in the run macro. The first ionisation collision (`e-G4DNAIonisation`) was then extracted with `sed -n '/ParentID = 0/,/e-G4DNAIonisation/p' G4OutputFileName.txt` and `grep` and `awk` were then used to extract the actual energy, `| grep "e-G4DNAIonisation" | awk '{print $5}'`

Figure 8: Gamma Simulation Agreement



ordinate axis). Non-linearity is observed for films less than 200 μm , this is evidence that the cascade electrons from the Compton electron are energetic enough that the range of the electrons is much greater than the thickness of the film and leave the film without colliding to an energy in which the energy deposition is linear (Figure 4).

$$\langle E \rangle = \frac{\int_0^\infty \phi(E) E dE}{\int_0^\infty \phi(E) dE} \text{ where} \quad (5.1)$$

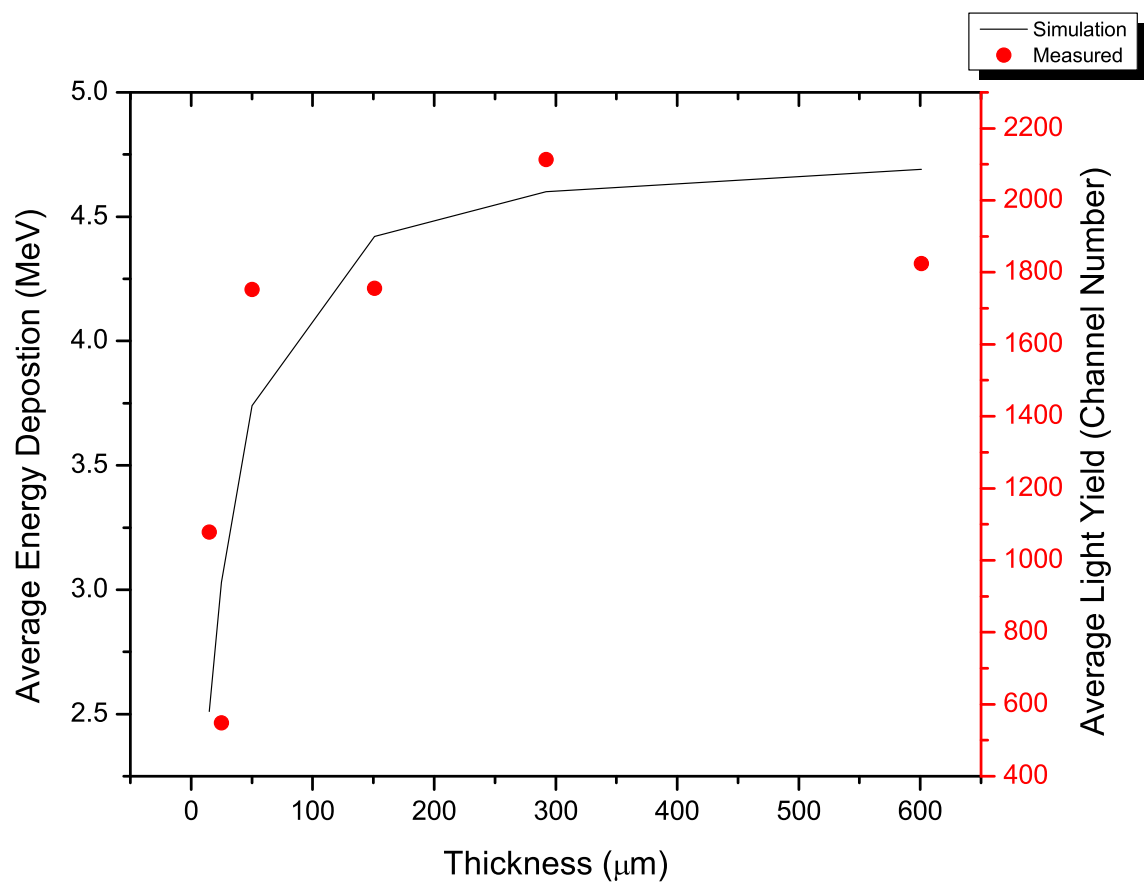
$$\langle \mu \rangle = \frac{\int_0^\infty f(x) x dx}{\int_0^\infty f(x) dx} \text{ where} \quad (5.2)$$

666

The comparison between the average energy deposition and measured channel allows for the a relationship to be drawn between the energy deposited and the channel number. This is completed by an taking an average of the ratio between the average channel number (Equation 5.2 and the average energy deposition (Equation 5.1). This ratio is defined in Equation 5.3. This quantity is defined seperately for neturons and gammas.

$$\eta = \sum_t \frac{\langle E \rangle}{\langle \mu \rangle} \quad (5.3)$$

Figure 9: Neutron Simulation Agreement



6 Results

6.1 Energy Deposition

The energy deposition was calculated for neutron and gamma events for films of thickness of 15 μm , 25 μm , 50 μm , 150 μm , 300 μm , 600 μm , 1 mm and 1 cm (Figure 10, 11).

Photons have a very low probability of interacting in the film due to polymer film being a low z-material. This is reflected in the majority of the events not interacting at all; about 1 in 10,000 of the events deposit energy in the film as seen in Figure 10. Several classic features of the spectra are apparent on the 1 cm thick film. These included the photo-peak in which all of the incident energy of the ^{60}Co is deposited in the film, as well as the individual Compton edges of the two photons from ^{60}Co . These features are not visible on the measured spectra due to the poor energy resolution of these films. There is also physical evidence of a lack of a Compton edge on the thinner films, but the films greater than 150 μm thick show some feature around 0.2 MeV. Films thinner than 150 μm show a very small amount of energy deposition that quickly tails off for higher energies, indicating that when a photon interaction occurs in the film the electrons from that interaction leave the film and the only energy deposition occurs from small ionizations as the highly energetic electron leaves the film material. It is also observed that the thinnest film (15 μm) has an average energy deposition of around 10 keV, while the 1 cm film has an average energy deposition of around 150 keV. The simulated energy deposition for neutron interactions in thin films is shown in Figure

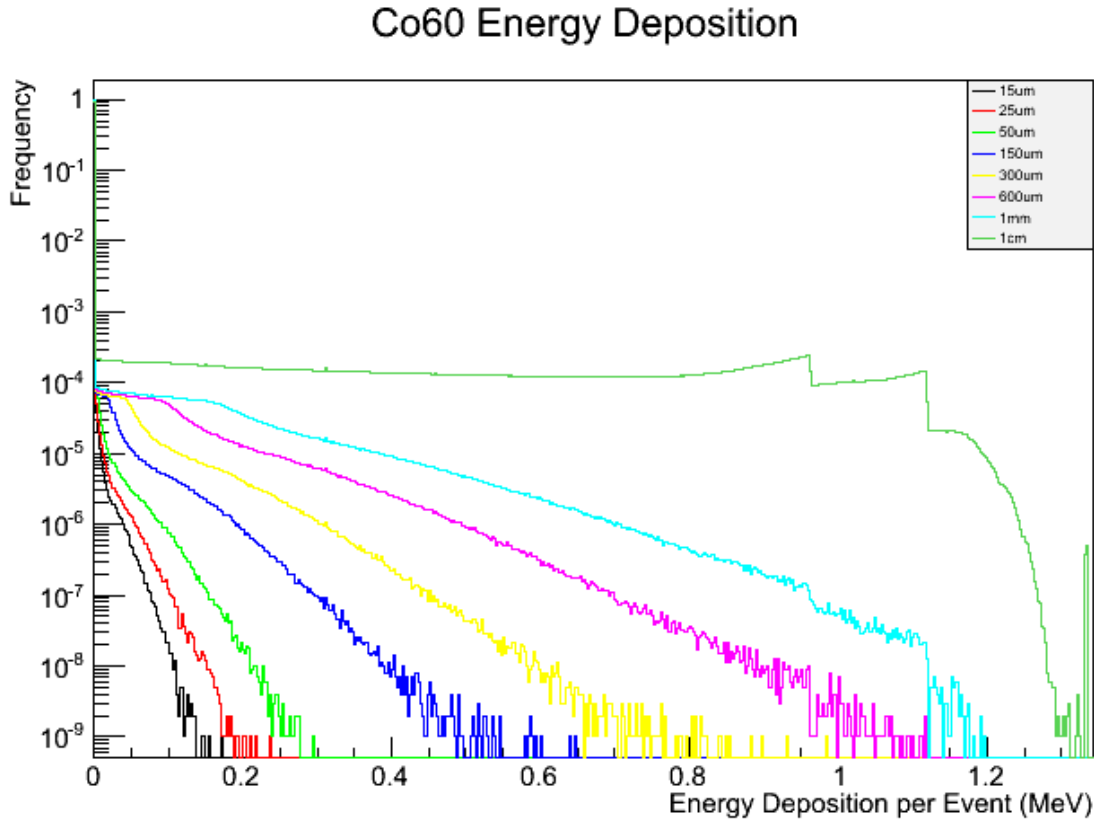


Figure 10: Simulated Energy Deposition for a Single Film (gammas)

11. Several features of the spectra can be immediately noted. For thick films (1 cm) there is a very high probability that a given event will deposit all of its energy in the film (as expected). Thinner films have a smaller probability of depositing all of their energy, but this is overshadowed by the thick samples when plotted. It is also interesting to note that it is possible to observe the comparative effects of the α and ^3H in the neutron energy deposition spectra. The triton has a much shorter range (10 μm in PS [12]) than the

689 α ($\sim 60 \mu\text{m}$) so it has a higher probability of depositing all of its energy. Thus, for energies above 2.73 MeV
 690 (the energy of the triton) there is a higher probability of energy energy deposition (by about a factor of 10).
 691 These events are still very infrequent compared to the probability of depositing all of the reaction product
 692 energy. Even for the $15 \mu\text{m}$ the average energy depositions was above 50% of the total Q-value of the reaction,
 and by $200 \mu\text{m}$ this average energy deposited approaches 95% of the total 4.78 MeV.

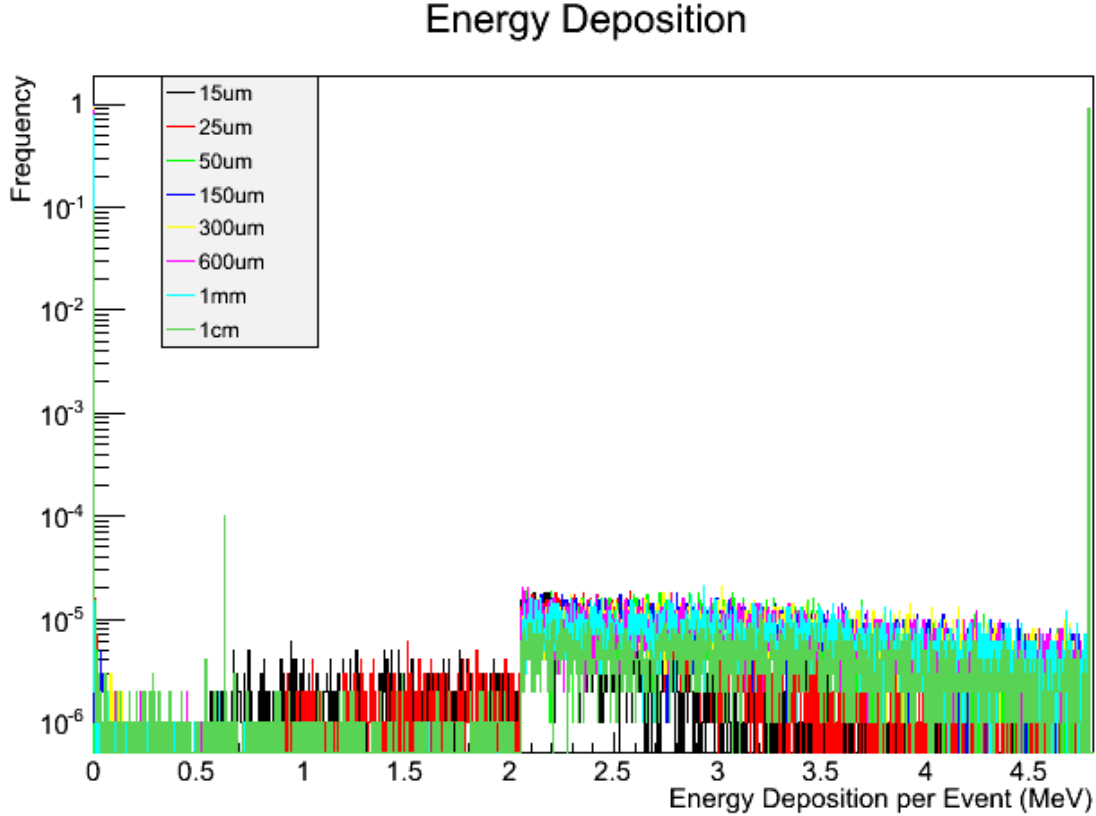
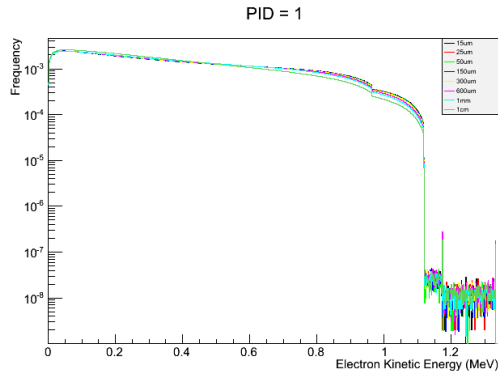


Figure 11: Simulated Energy Deposition for a Single Film (neutrons)

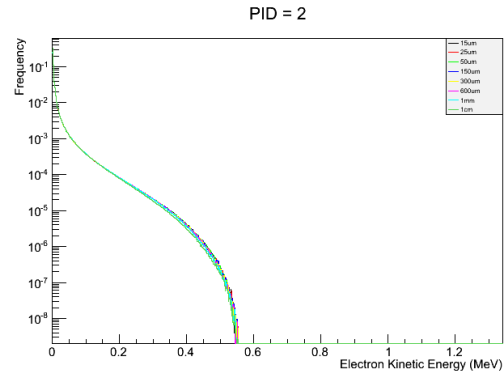
693

6.2 Secondary Electron Energy Distribution

695 The distribution of secondary electrons from photon interactions are plotted in Figure 12. From these results
 696 it can be concluded that it is unlikely (around 1 in 10,000) that an electron will be scattered with the
 697 maximum Compton scattering kinetic energy, but rather have an energy somewhat lower than that. The
 698 distribution of secondary electrons from photon interactions is actually very flat, implying that it is likely
 699 for the electron from a Compton scattering event to have an energy in the 100's of keV. The distribution of
 700 the next generation of electrons was also calculated, and this distribution was also quite energetic (with a
 701 maximum energy corresponding to 0.55 MeV) but with a much larger probability of having a collision that
 702 produces an electron with a much lower energy.



(a) First Secondary Electron



(b) Second Secondary Electron

Figure 12: Simulated kinetic energies of electrons from ^{60}Co interactions

7 Conclusions

GEANT4 has been employed to simulate the energy spectra of electrons and energy deposition from thermal neutrons and ^{60}Co gammas. A versatile implementation of the geometry was used in which it is possible to dynamically set the materials, thickness, and number of layers between runs. In addition, analysis methods have been written to aid in the reporting of the results. This simulation was verified by reproducing the single collision energy loss spectra for water, and also by comparing the average energy deposited to the measured average channel number for film ranging from $15\mu\text{m}$ to $600\mu\text{m}$.

The energy deposition of the films were calculated and plotted in Figure 11 and Figure 10. It is then observable that the gamma interactions have a very low probability of depositing a majority of the energy from a ^{60}Co photon into the material, while neutrons tend to deposit over 50% of their energy in the material for a $15\mu\text{m}$ film, and increasing to 96% for a 1 cm thick film. Figure 13 shows the average energy deposition as a function of thickness for neutrons and gammas, along with the calculated channel number (according to Equation 5.3). At thickness of less than $200\mu\text{m}$ there is significant separation between the average energy deposited by neutron events compared to gamma events. As the thickness of the films increased the average neutron energy approached the asymptotic limit of 4.78 MeV, while the average gamma energy increased. This creates less separation between the two, and provides less of an ability for neutron-gamma discrimination based on pulse height.

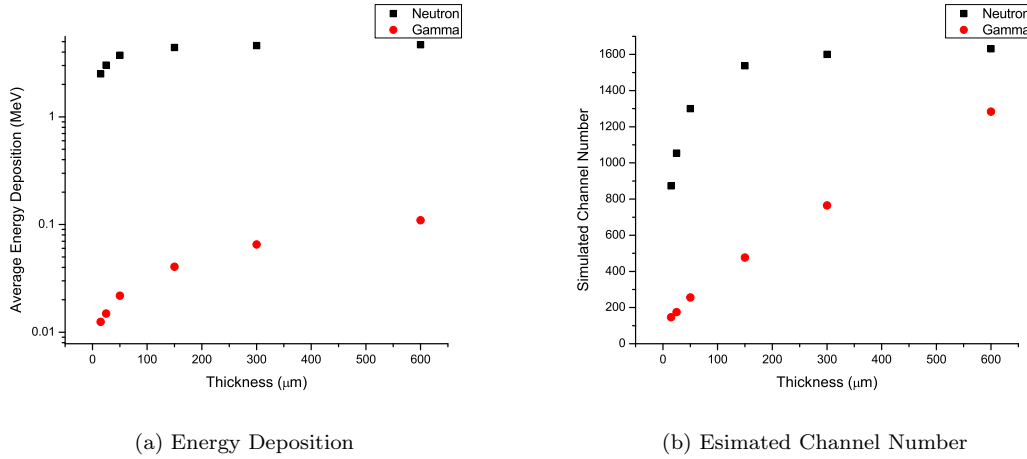


Figure 13: Comparison between average neutron and gamma energy deposition

References

- [1] CPB, “On a typical day in fiscal year 2011 CBP.” <http://www.cbp.gov/xp/cgov/about/>, 2012.
- [2] R. T. Kouzes, J. H. Ely, L. E. Erikson, W. J. Kernan, A. T. Lintereur, E. R. Siciliano, D. L. Stephens, D. C. Stromswold, R. M. Van Ginhoven, and M. L. Woodring, “Neutron detection alternatives to ^3He for national security applications,” *Nuclear Instruments and Methods in Physics Research Section A: Accelerators, Spectrometers, Detectors and Associated Equipment*, vol. 623, pp. 1035–1045, Nov. 2010.
- [3] R. Kouzes, J. Ely, A. Lintereur, and D. Stephens, “Neutron detector gamma insensitivity criteria,” *PNNL 18903*, 1999.
- [4] J. E. Turner, H. G. Paretzke, R. N. Hamm, H. A. Wright, and R. H. Ritchie, “Comparative study of electron energy deposition and yields in water in the liquid and vapor phases,” *Radiation Research*, vol. 92, pp. 47–60, Oct. 1982. ArticleType: research-article / Full publication date: Oct., 1982 / Copyright 1982 Radiation Research Society.
- [5] S. Agostinelli, J. Allison, K. Amako, J. Apostolakis, H. Araujo, P. Arce, M. Asai, D. Axen, S. Banerjee, G. Barrand, F. Behner, L. Bellagamba, J. Boudreau, L. Broglia, A. Brunengo, H. Burkhardt, S. Chauvie, J. Chuma, R. Chytrcek, G. Cooperman, G. Cosmo, P. Degtyarenko, A. Dell’Acqua, G. Depaola, D. Dietrich, R. Enami, A. Feliciello, C. Ferguson, H. Fesefeldt, G. Folger, F. Foppiano, A. Forti, S. Garelli, S. Giani, R. Giannitrapani, D. Gibin, J. Gomez Cadenas, I. Gonzalez, G. Gracia Abril, G. Greeniaus, W. Greiner, V. Grichine, A. Grossheim, S. Guatelli, P. Gumplinger, R. Hamatsu, K. Hashimoto, H. Hasui, A. Heikkinen, A. Howard, V. Ivanchenko, A. Johnson, F. Jones, J. Kallenbach, N. Kanaya, M. Kawabata, Y. Kawabata, M. Kawaguti, S. Kelner, P. Kent, A. Kimura, T. Kodama, R. Kokoulin, M. Kossov, H. Kurashige, E. Lamanna, T. Lampn, V. Lara, V. Lefebure, F. Lei, M. Liendl, W. Lockman, F. Longo, S. Magni, M. Maire, E. Medernach, K. Minamimoto, P. Mora de Freitas, Y. Morita, K. Murakami, M. Nagamatsu, R. Nartallo, P. Nieminen, T. Nishimura, K. Ohtsubo, M. Okamura, S. O’Neale, Y. Oohata, K. Paech, J. Perl, A. Pfeiffer, M. Pia, F. Ranjard, A. Rybin, S. Sadilov, E. Di Salvo, G. Santin, T. Sasaki, N. Savvas, Y. Sawada, S. Scherer, S. Sei, V. Sirotenko, D. Smith, N. Starkov, H. Stoecker, J. Sulkimo, M. Takahata, S. Tanaka, E. Tcherniaev, E. Safai Tehrani, M. Tropeano, P. Truscott, H. Uno, L. Urban, P. Urban, M. Verderi, A. Walkden, W. Wander, H. Weber, J. Wellisch, T. Wenaus, D. Williams, D. Wright, T. Yamada, H. Yoshida, and D. Zschesche, “Geant4a simulation toolkit,” *Nuclear Instruments and Methods in Physics Research Section A: Accelerators, Spectrometers, Detectors and Associated Equipment*, vol. 506, pp. 250–303, July 2003.
- [6] G. Collaboration, “Geant4 user’s guide for application developers.” <http://geant4.web.cern.ch/geant4/UserDocumentation/UsersGuides/ForApplicationDeveloper/html/index.html>, Dec. 2011. Version geant4 9.5.0.
- [7] J. Allison, K. Amako, J. Apostolakis, H. Araujo, P. Dubois, M. Asai, G. Barrand, R. Capra, S. Chauvie, R. Chytrcek, G. Cirrone, G. Cooperman, G. Cosmo, G. Cuttone, G. Daquino, M. Donszelmann, M. Dressel, G. Folger, F. Foppiano, J. Generowicz, V. Grichine, S. Guatelli, P. Gumplinger, A. Heikkinen, I. Hrivnacova, A. Howard, S. Incerti, V. Ivanchenko, T. Johnson, F. Jones, T. Koi, R. Kokoulin, M. Kossov, H. Kurashige, V. Lara, S. Larsson, F. Lei, O. Link, F. Longo, M. Maire, A. Mantero, B. Mascialino, I. McLaren, P. Lorenzo, K. Minamimoto, K. Murakami, P. Nieminen, L. Pandola, S. Parlati, L. Peralta, J. Perl, A. Pfeiffer, M. Pia, A. Ribon, P. Rodrigues, G. Russo, S. Sadilov, G. Santin, T. Sasaki, D. Smith, N. Starkov, S. Tanaka, E. Tcherniaev, B. Tome, A. Trindade, P. Truscott, L. Urban, M. Verderi, A. Walkden, J. Wellisch, D. Williams, D. Wright, and H. Yoshida, “Geant4 developments and applications,” *Nuclear Science, IEEE Transactions on*, vol. 53, pp. 270–278, Feb. 2006.
- [8] CERN, “Physics lists EM constructors in geant4 9.3.” <http://geant4.cern.ch/geant4/collaboration/working-groups/electromagnetic/physlist9.3.shtml>, Feb. 2012.
- [9] CERN, “Reference physics lists.” http://geant4.cern.ch/support/proc_mod_catalog/physics_lists/referencePL.shtml, Oct. 2008.

767
768

[10] CERN, “Detector definition and response.” <http://geant4.web.cern.ch/geant4/UserDocumentation/UsersGuides/ForApplicationDeveloper/html/index.html>, 2012.

769
770

[11] J. B. Birks, “Scintillations from organic crystals: Specific fluorescence and relative response to different radiations,” *Proceedings of the Physical Society. Section A*, vol. 64, pp. 874–877, Oct. 1951.

771
772
773

[12] H. Kudo and K. Tanaka, “Recoil ranges of 2.73 MeV tritons and yields of ^{18}F produced by the $^{16}\text{O}(\text{t},\text{n})^{18}\text{F}$ reaction in neutron-irradiated lithium compounds containing oxygen,” *The Journal of Chemical Physics*, vol. 72, no. 5, p. 3049, 1980.

GEANT4 Implementation

Visible light in GEANT4 is known as an optical photon. An optical photon has momentum ($\vec{p} = \hbar\vec{k}$), corresponding to the energy and direction of the photon, as well as a polarization (\vec{e}). The GEANT4 toolkit breaks up light transport into two parts; the creation of the optical photon and the transport of the optical photon through the material. Each of these are material dependent properties which need to be supplied by the user. This is done by creating a material properties table `G4MaterialPropertyTable`, of which the following properties are available:

- `RINDEX`
- `ABSLENGTH`

Scintillation Process

The number of optical photons generated by GEANT4 is proportional to the energy lost during the step, determining the energy from the empirical emission spectra of the material. In GEANT4 this is accomplished by creating a `G4Scintillation` process.⁶

```
#include "G4Scintillation.hh"

G4Scintillation* theScintProcess = new G4Scintillation("Scintillation");

theScintProcess->SetTrackSecondariesFirst(true);
theScintProcess->SetScintillationYield(7500.0/MeV);
theScintProcess->SetResolutionScale(1.0);
theScintProcess->SetScintillationTime(45.*ns);
```

Optical Photon Transport

There are three classes of optical photon interactions in GEANT4:

- Refraction and reflection
- Bulk Absorption
- Rayleigh scattering

Of these only refraction and reflection are necessary. [?]

⁶As the scintillation properties are attached to the process and not the material. GEANT4 is incapable of more than one scintillation material in any given application.